

Tropism of SARS-CoV-2, SARS-CoV, and Influenza Virus in Canine Tissue Explants

Christine H. T. Bui,¹ Hin Wo Yeung,¹ John C. W. Ho,¹ Connie Y. H. Leung,² Kenrie P. Y. Hui,¹ Ranawaka A. P. M. Perera,¹ Richard J. Webby,³ Stacey L. Schultz-Cherry,³ John M. Nicholls,⁴ Joseph Sriyal Malik Peiris,¹ and Michael C. W. Chan^{1,6}

¹School of Public Health, Li Ka Shing Faculty of Medicine, The University of Hong Kong, Hong Kong Special Administrative Region, China, ²Centre for Comparative Medicine Research, Li Ka Shing Faculty of Medicine, The University of Hong Kong, Hong Kong Special Administrative Region, China, ³Department of Infectious Diseases, St. Jude Children's Research Hospital, Memphis, Tennessee, USA, and ⁴Department of Pathology, Queen Mary Hospital, Li Ka Shing Faculty of Medicine, The University of Hong Kong, Hong Kong Special Administrative Region, China

Background. Human spillovers of severe acute respiratory syndrome coronavirus 2 (SARS-CoV-2) to dogs and the emergence of a highly contagious avian-origin H3N2 canine influenza virus have raised concerns on the role of dogs in the spread of SARS-CoV-2 and their susceptibility to existing human and avian influenza viruses, which might result in further reassortment.

Methods. We systematically studied the replication kinetics of SARS-CoV-2, SARS-CoV, influenza A viruses of H1, H3, H5, H7, and H9 subtypes, and influenza B viruses of Yamagata-like and Victoria-like lineages in ex vivo canine nasal cavity, soft palate, trachea, and lung tissue explant cultures and examined ACE2 and sialic acid (SA) receptor distribution in these tissues.

Results. There was limited productive replication of SARS-CoV-2 in canine nasal cavity and SARS-CoV in canine nasal cavity, soft palate, and lung, with unexpectedly high ACE2 levels in canine nasal cavity and soft palate. Canine tissues were susceptible to a wide range of human and avian influenza viruses, which matched with the abundance of both human and avian SA receptors.

Conclusions. Existence of suitable receptors and tropism for the same tissue foster virus adaptation and reassortment. Continuous surveillance in dog populations should be conducted given the many chances for spillover during outbreaks.

Keywords. COVID-19; SARS-CoV-2; SARS-CoV; influenza; dogs; ex vivo; explants.

Dogs are called man's best friend, offering companionship, services, loyalty, and love to their human counterparts. According to the 2019–2020 American Pet Products Association national pet owners survey, over 50% of US households own a pet dog. Many consider their dogs to be members of the family and sleep next to them on their beds [1]. However, eating dog meat is also normal in many countries, including China, South Korea, and Vietnam.

In the context of the close and complicated relationships between dogs and humans, zoonosis and reverse zoonosis become a concern. Recently, the isolation of severe acute respiratory syndrome coronavirus 2 (SARS-CoV-2) from a pet dog in Hong Kong has raised concern about the possible role of dogs in SARS-CoV-2 transmission [2]. Furthermore, the emergence of a highly contagious avian-origin H3N2 canine influenza virus in South Korea [3, 4] and China [5], and its rapid geographical expansion to places like the United States [6] and Canada [7], have brought fear of both the zoonotic potential of the virus and the susceptibility of dogs to a wide variety of human and

avian influenza viruses, which historically caused seasonal epidemics and periodic unpredictable pandemics in humans. Serological surveys of human H1N1 and H3N2 seasonal and 2009 H1N1 pandemic (2009 H1N1 pdm) viruses in pet dogs showed seroprevalence between 1.2% and 9.5% [8–10], providing evidence of past infection. With swine being historically considered a “mixing vessel” for influenza viruses [11, 12], any animals, including dogs, can potentially be mixing vessels in addition to swine if they are similarly susceptible to infection with both human and avian influenza viruses. Replication in dogs provides a chance for viruses to amplify, mutate, and reassort, thus facilitating cross-species transmission and the emergence of new viruses with potential threat to public health. Therefore, understanding the ability of these viruses to replicate in dogs is important in unveiling past events and prevent future outbreaks through appropriate prevention and control methods.

Similar to the use of ex vivo human respiratory explant cultures to investigate viral tropism and pathogenesis [13–15], we utilize tissue explants of canine nasal cavity, soft palate, trachea, and lung to systematically risk assess the susceptibility of dogs to the infection of currently pandemic, circulating, and of public health concern coronaviruses and influenza viruses, including SARS-CoV-2, SARS-CoV, human and avian influenza A viruses (IAVs) of H1, H3, H5, H7, and H9 subtypes, and influenza B viruses (IBVs) of Yamagata-like and Victoria-like lineages, in an attempt to better understand the role of dogs in the epidemiology of these emerging infectious viruses.

Received 19 October 2020; editorial decision 30 December 2020; accepted 4 January 2021; published online January 4, 2021.

Correspondence: M. C. W. Chan, PhD, L6-39 6/F Laboratory Block, Faculty of Medicine Building, 21 Sassoon Road, Pokfulam, Hong Kong SAR, China (mchan@hku.hk).

The Journal of Infectious Diseases® 2021;224:821–30

© The Author(s) 2021. Published by Oxford University Press for the Infectious Diseases Society of America. All rights reserved. For permissions, e-mail: journals.permissions@oup.com. DOI: 10.1093/infdis/jjab002

METHODS

Viruses

We used: SARS-CoV-2 (BetaCoV/HongKong/VM20001061/2020 and SARS-CoV-2/canine/HKG/20-03695/2020), isolated from the nasopharyngeal aspirate and throat swab of a confirmed coronavirus disease 2019 (COVID-19) patient in Hong Kong in January 2020 [14] and the nasal swab of an infected German Shepherd pet dog in Hong Kong in March 2020, [2] respectively; SARS-CoV (strain HK39849), isolated from a hospitalized patient in Hong Kong in 2003; 2009 H1N1 pdm (A/California/04/2009); canine and human seasonal H3N2 (A/canine/Illinois/41915/2015 and A/Bethesda/55/2015) [16]; highly pathogenic avian influenza (HPAI) H5N1 (A/HongKong/483/1997), isolated from a fatal human case in Hong Kong; HPAI H5N6 (A/Guangzhou/39715/2014), isolated from the throat swab of a hospitalized patient; HPAI H5N8 (A/Chicken/Egypt/F1366A/2017); HPAI H7N9 (A/Guangdong/17SF006/2017), isolated from a fatal case during the fifth epidemic wave in China; Madin-Darby canine kidney (MDCK) cell-passaged high cytokine variant of H9N2 (A/Quail/HongKong/G1/1997), with an asparagine (N) instead of aspartic acid (D) at position 253 and a lysine (K) instead of glutamine (Q) at position 591 of the PB2 protein [17]; Yamagata-like IBV (B/Taiwan/N1902/2004); and Victoria-like IBV (B/HongKong/38551/2005). Virus stocks of SARS-CoV-2 and SARS-CoV were prepared and titrated in VeroE6 cells, while those of IAVs and IBVs were prepared and titrated in MDCK cells. Virus titers were determined using 50% tissue culture infection dose (TCID₅₀) and plaque assays (see [Supplementary Methods](#)).

All infection experiments were done in a biosafety level 3 facility at the School of Public Health, Li Ka Shing Faculty of Medicine, The University of Hong Kong, Hong Kong SAR, China.

Isolation and Culture of Canine Explants

Carcasses of apparently healthy stray/abandoned mongrel dogs of both sexes in Hong Kong were collected from the pounds shortly after being euthanized with xylazine and ketamine combination and an overdose of sodium pentobarbital injection. The dogs were not sacrificed for the purpose of our experiments but were diagnosed to have serious temperament issues or problems and could not be rehomed. The dogs were adults but the ages were not known due to technical difficulties. Nasal and tracheal swabs were collected for the quantitative polymerase chain reaction (qPCR) detection of SARS-CoV ORF1b gene, IAV matrix gene, and IBV haemagglutinin gene (see [Supplementary Methods](#)). Only data sets with negative qPCR results were used for analysis.

Nasal Cavity Explants

The outer skin of the external nose was peeled off and the inner cartilaginous structure was excised and rinsed in washing medium containing phosphate buffered saline (PBS), pH 7.4, 1000 U/mL penicillin, 1000 µg/mL streptomycin, 0.5 mg/mL gentamicin, and 0.25 µg/mL amphotericin B (all Gibco). Any excessive tissue on the outside of the cartilaginous frame was removed before the 2 nasal cavities were cut open. The inner epithelium attached to the cartilage was sectioned into square explants of approximately 5 mm in length. Explants were put on surgical sponges (Simport) with the epithelial surface facing upward in nasal cavity-trachea culture medium containing a 1:1 mixture of RPMI 1640 and DMEM, high glucose, 100 U/mL penicillin, 100 µg/mL streptomycin, 0.1 mg/mL gentamicin, and 2 mM L-glutamine (all Gibco), thus creating an air-liquid interface.

Soft Palate Explants

The soft palate was obtained from an opening at the throat. After rinsing in washing medium, tissue at the nasopharyngeal side was removed leaving behind the oral epithelium with minimum connective tissues. The epithelium was sectioned into square explants and put on surgical sponges, as for nasal cavity explants, and cultured in soft palate culture medium containing Ham's F-12K (Kaighn's) medium, 100 U/mL penicillin, 100 µg/mL streptomycin, and 0.1 mg/mL gentamicin (all Gibco).

Trachea Explants

The middle part of the tracheal tube was excised from the respiratory tract, rinsed in washing medium, and cut open. The epithelium attached to cartilage was cut into square explants, put on surgical sponges and cultured in nasal cavity-trachea culture medium, as for nasal cavity explants.

Lung Explants

The tips of lung lobes of approximately 5 mm in depth were excised, cut into triangular sheets of around 1 mm thick, rinsed with washing medium, and cultured in lung culture medium containing Ham's F-12K (Kaighn's) medium, 100 U/mL penicillin, and 100 µg/mL streptomycin (all Gibco).

The above methods were adopted from previous studies with modifications [13, 18, 19].

Infection of Canine Explants

Within 3 hours after isolation, canine explants were submerged in 1 mL of approximately 1×10^6 plaque-forming units (PFU)/mL virus for 1 hour in a humidified incubator at 37°C (nasal cavity, soft palate, and trachea explants) or 38.5°C (lung explants) and 5% CO₂. After infection, explants were washed 3 times with PBS, pH 7.4 (Gibco), to remove unbound viruses. Each piece of nasal cavity, soft palate, and trachea explants was put on a surgical sponge (Simport) floating on 1.5 mL of nasal

cavity-trachea or soft palate culture medium, accordingly. They were maintained in a humidified incubator at 37°C and 5% CO₂. Lung explants were similarly maintained in lung culture medium but without surgical sponges and kept at 38.5°C, which is a physiologically relevant temperature. Culture supernatant was collected at 1, 24, 48, 72, and 96 hours postinfection (hpi) for virus titration by TCID₅₀ assays. Experiments were performed with tissues from 3 or more dogs.

Histochemical Staining

Canine tissues were fixed in 10% neutral-buffered formalin immediately after isolation and later paraffin embedded. Formalin-fixed paraffin-embedded tissue sections were deparaffinized in xylene and rehydrated in graded alcohols, 100%, 95%, and 80%, for subsequent processing.

Angiotensin-Converting Enzyme 2

Tissue sections were microwaved at 95°C in 10 mM citrate buffer pH 6.0 for 15 minutes, blocked with normal horse serum at room temperature (RT) for 10 minutes, and incubated with 1:50 rabbit polyclonal ACE2 antibody-middle region (Aviva Systems Biology) at RT for 1 hour followed by ImmPRESS HRP Horse Anti-Rabbit IgG Polymer Detection Kit, Peroxidase (Vector Laboratories) at RT for 1 hour. The sections were developed with Vector NovaRED Substrate Kit, Peroxidase (HRP) (Vector Laboratories) for 3 minutes at RT.

Lectins

Tissue sections were microwaved at 95°C in 10 mM citrate buffer pH 6.0 for 10 minutes, blocked with 0.05% bovine serum albumin at RT for 10 minutes, and incubated with 1:100 biotinylated *Sambucus nigra* lectin (SNA), *Maackia amurensis* lectin I (MAAI), or *Maackia amurensis* lectin II (MAAII) (Vector Laboratories) at RT for 1 hour followed by 1:100 streptavidin, alkaline phosphatase (Vector Laboratories) at RT for 45 minutes. The sections were developed with Vector Red Substrate Kit, Alkaline Phosphatase (AP) (Vector Laboratories) at RT for 5–15 minutes.

Mayer's hematoxylin was used to counterstain the nuclei in all tissue sections for 1 minute. The sections were blued with Scott's tap water, air dried, and mounted with Permount (Fisher Scientific).

Statistical and Sequencing Analysis

Area under the curve (AUC) calculation and statistical analysis were performed using GraphPad Prism, version 8.4.3. AUC values represented the areas under the replication kinetic curves from 24 to 72 hpi above the TCID₅₀ assay detection limit (1.5 log TCID₅₀/mL) calculated using the trapezoid rule. AUC values were compared by 1-way analysis of variance (1-way ANOVA), with Bonferroni posttests.

Sequence alignment and analysis were carried out in MEGA, version 7.0.21. Nucleotide sequences of BetaCoV/

HongKong/VM20001061/2020 and SARS-CoV-2/canine/HKG/20-03695/2020 used for amino acid sequence analysis were obtained from GISAID, EPI_ISL_412028 and GENBANK, MT270814.

RESULTS

Limited Productive Replication of SARS-CoV-2 and SARS-CoV in Canine Nasal Cavity Explants

Consistent with the in vivo challenge study of SARS-CoV-2 in beagles [20], both human and canine isolates of SARS-CoV-2 in our study replicated poorly in the 4 canine explant systems (Figure 1). There was limited productive replication in nasal cavity explants, with virus titers in the culture supernatant reaching 3.1 to 3.2 log TCID₅₀/mL by 96 hpi, which may correspond in part to the low positive sporadic detection of SARS-CoV-2 in canine nasal swabs [2]. Replication in other explants remained minimal or undetected. Although the 2 SARS-CoV-2 isolates were clearly distinguishable with 7 amino acid difference (Table 1), including position 614 (D/G) of the spike protein where G614 in the canine isolate was associated with higher viral loads in humans [21], we did not observe any obvious differences in viral fitness in canine explants. Similarly, we only observed limited productive replication of SARS-CoV in canine nasal cavity, soft palate, and lung explants, with peak virus titers between 3.6 and 4.0 log TCID₅₀/mL at 72 to 96 hpi (Figure 1). Trachea explants remained nonpermissive to SARS-CoV.

Abundance of ACE2 Receptors in Canine Nasal Cavity and Soft Palate Epithelia

Staining for ACE2, the entry receptor for SARS-CoV-2 and SARS-CoV, revealed abundant expressions in canine nasal cavity and soft palate epithelia, with the most intense staining in the middle and bottom cell layers, respectively (Figure 2). In canine trachea and lung epithelia, ACE2 expressions ranged from rare to mild.

Efficient Replication of Different Influenza Subtypes in Canine Tissue Explants

Influenza viruses of different subtypes readily infected and replicated in the canine tissue explants (Figure 3). Canine H3N2, being highly contagious in dogs, replicated efficiently in nasal cavity, trachea, and lung explants, producing peak virus titers as high as 6.6 log TCID₅₀/mL within 72 hpi (Figure 3A). Among the 7 human/avian IAV subtypes and 2 IBV isolates, HPAI H5N1, H5N6, and H7N9 and quail H9N2 replicated most efficiently in nasal cavity explants. They shared comparable areas under their replication kinetic curves (AUC) from 24 to 72 hpi with that of canine H3N2 (Figure 3B). The means of their peak virus titers from 24 to 72 hpi ranged between 4.7 and 5.7 log TCID₅₀/mL while those of the least efficient IBVs were 2.6 to 2.7 log TCID₅₀/mL. In soft palate explants, HPAI H5N1, H5N6, and H7N9 remained the most replicative viruses, with the

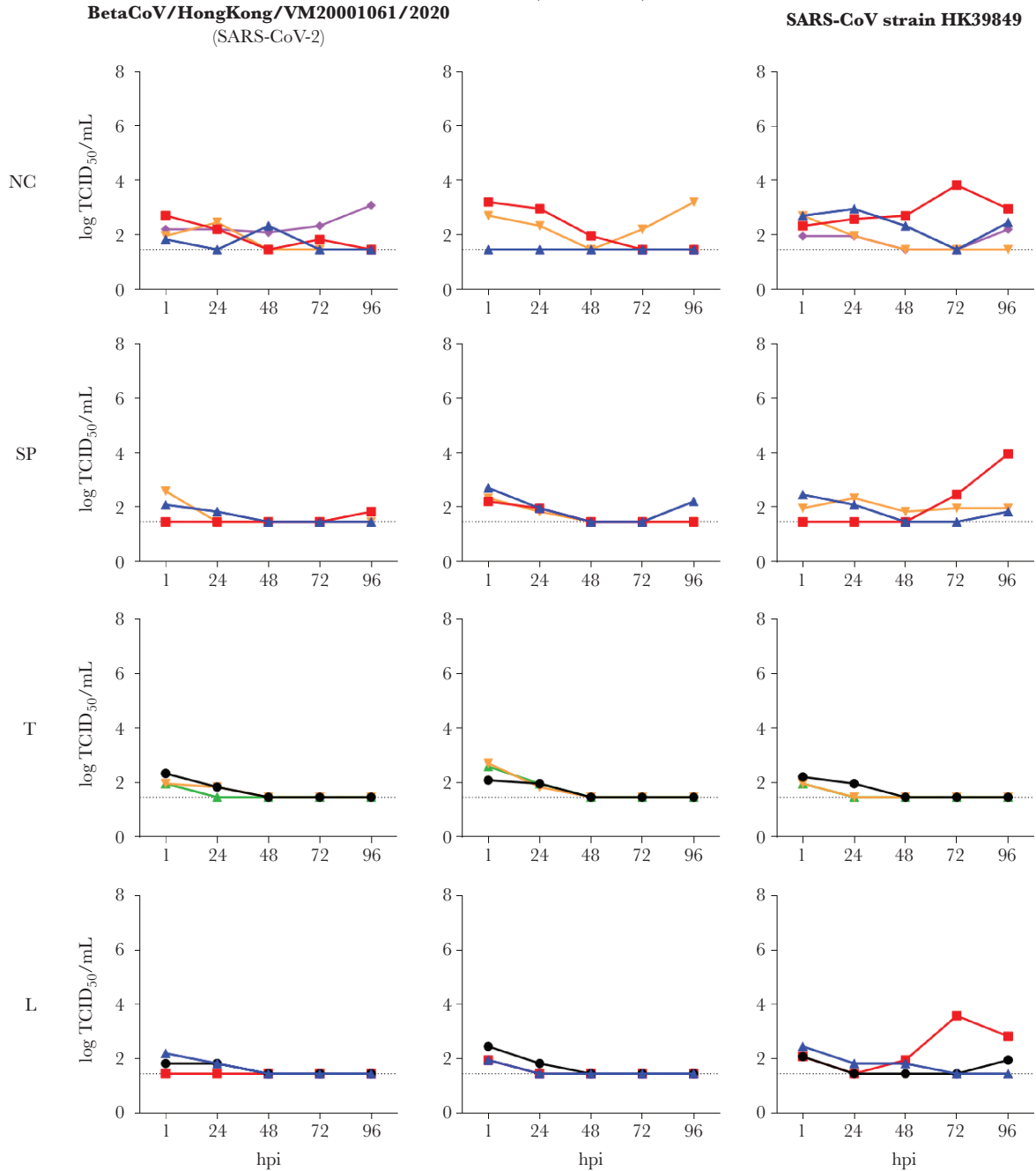


Figure 1. Replication kinetics of SARS-CoV-2 and SARS-CoV in canine tissue explants. Explants were infected with approximately 1×10^6 PFU/mL virus. Virus titers in the culture supernatant at 1, 24, 48, 72, and 96 hpi were determined by TCID₅₀ assay with a detection limit of 1.5 log TCID₅₀/mL, denoted by the dotted lines. Each column shows the replication kinetics per virus strain. Each row displays the results per explant system. Each line color represents data from an individual dog in a single replicate. Experiments were done using tissues from at least 3 different dogs. Abbreviations: hpi, hours postinfection; L, lung; NC, nasal cavity; PFU, plaque-forming unit; SARS-CoV-2, severe acute respiratory syndrome coronavirus 2; SP, soft palate; T, trachea; TCID₅₀, 50% tissue culture infection dose.

means of their peak virus titers reaching 5.1 to 6.2 log TCID₅₀/mL and AUC values being statistically higher than that of canine H3N2. Canine H3N2, 2009 H1N1 pdm, HPAI H5N8, and quail H9N2 showed slightly productive replication with the means of their peak virus titers at 3.2 to 3.5 log TCID₅₀/mL.

Replication of human seasonal H3N2 and IBVs were mainly at marginal or undetected levels. In trachea explants, the AUC values of all human/avian IAVs and IBVs were statistically lower than that of canine H3N2. However, except for human seasonal H3N2 and Victoria-like IBV, the means of their peak

Table 1. Amino Acid Differences Between the Human and Canine SARS-CoV-2 Isolates

Protein	Position	Amino Acid		Significance
		Human Isolate ^a	Canine Isolate ^b	
ORF1ab polyprotein/RNA-dependent RNA polymerase (nsp12)	4715	P	L	L4715 [22] Higher fatality rate
Spike glycoprotein	367	F	V	Within receptor binding domain [23].
	614	D	G	G614 [21, 22] Current dominant pandemic form Higher viral loads in patients Higher fatality rate
ORF8 protein	62	L	V	...
	84	S	L	...
Nucleocapsid phosphoprotein	203	R	K	Within serine-arginine-rich motif involved in viral capsid formation [24]
	204	G	R	

^aBetaCoV/HongKong/VM20001061/2020 (GISAID accession number EPI_ISL_412028).

^bSARS-CoV-2/canine/HKG/20-03695/2020 (GENBANK accession number MT270814).

virus titers were all ≥ 3.6 log TCID₅₀/mL. Those of HPAI H5N6 and H7N9 and quail H9N2 reached 4.9 to 5.1 log TCID₅₀/mL, which is only around 1 log lower than that of canine H3N2. In lung explants, human/avian IAVs, Victoria-like IBV, and canine H3N2 showed comparable AUC values with the means of their peak virus titers ranging between 4.5 and 5.7 log TCID₅₀/mL. Yamagata-like IBV yielded peak virus titers between the undetected level (≤ 1.5 log TCID₅₀/mL) and 3.3 log TCID₅₀/mL.

Abundance of α 2,3- and α 2,6-Linked Sialic Acid Receptors in Canine Respiratory and Soft Palate Epithelia

To determine the sialic acid (SA) receptor distribution in the canine tissues, we performed lectin histochemistry. SNA binding

(specific towards α 2,6-linked SA) was abundant in the epithelia of nasal cavity, trachea, and bronchioles, but moderate in soft palate and alveolus (Figure 4). The MAAI and MAII isotypes, which preferentially bind N-linked or core 2 O-linked glycans containing SA α 2,3-Gal β 1,4GlcNAc, and O-linked glycans containing SA α 2,3-Gal β 1,3GalNAc, respectively [25, 26], displayed distinct distribution patterns. MAAI binding was abundant in the epithelia of soft palate and bronchioles, moderate at the level of nasal cavity, and rare in trachea and alveolus. MAII binding was abundant in the epithelia of all tissue explants. Note that MAAI and MAII are also known to bind with high affinity to non-SA glycans containing SO₄-3-Gal β 1,4GlcNAc and SO₄-3-Gal β , respectively [25, 26].

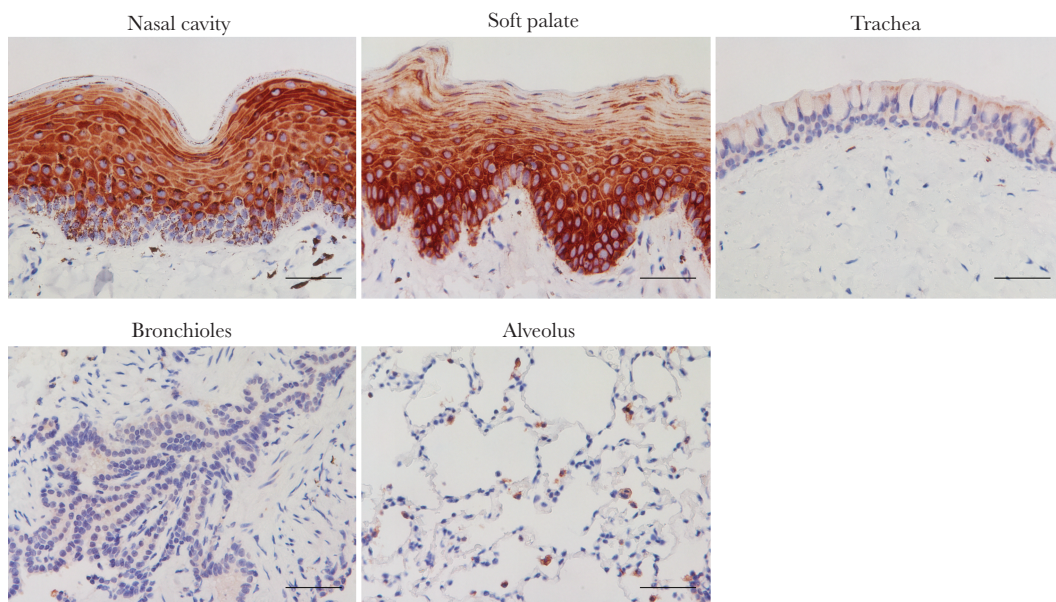


Figure 2. Angiotensin-converting enzyme 2 (ACE2) receptor distribution in canine respiratory and soft palate tissues. Immunohistochemical staining for ACE2 (brown) in 10% formalin-fixed paraffin-embedded canine nasal cavity, soft palate, trachea, and lung (bronchioles and alveolus) tissue explants. Scale bars = 50 μ m.

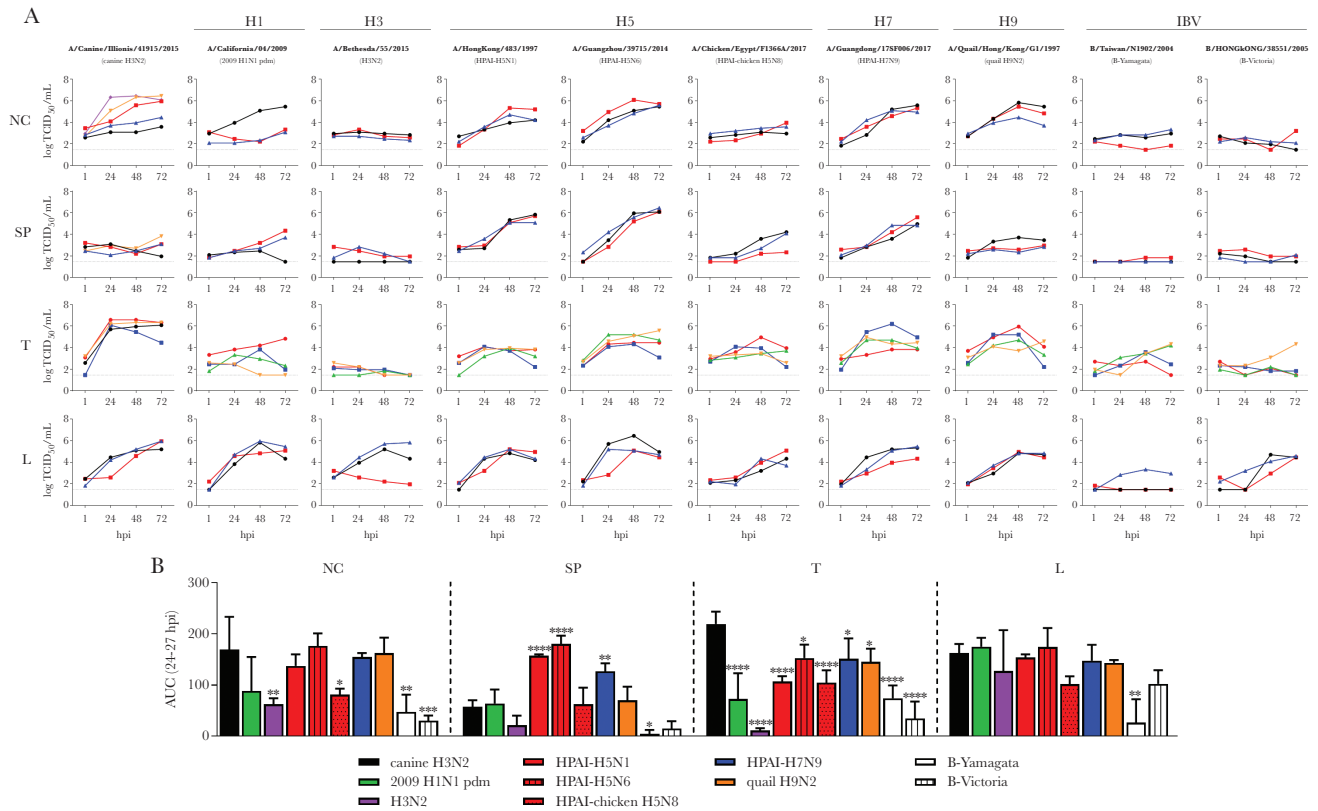


Figure 3. Replication kinetics of IAVs and IBVs in canine tissue explants. *A*, Explants were infected with 1×10^6 PFU/mL virus. Virus titers in the culture supernatant at 1, 24, 48, and 72 hpi were determined by TCID₅₀ assay with a detection limit of 1.5 log TCID₅₀/mL, denoted by the dotted lines. Each column shows the replication kinetics per virus strain. Each row displays the results per explant system. Each line color represents data from an individual dog in a single replicate. Experiments were done using tissues from at least 3 different dogs. *B*, AUC above the TCID₅₀ detection limit was calculated from the virus titers at 24 to 72 hpi (mean \pm SD). Statistical significance between AUC values of canine H3N2 compared to other viruses in each explant system was analyzed using 1-way ANOVA with Bonferroni posttests. * $P \leq .05$, ** $P \leq .01$, *** $P \leq .001$, **** $P \leq .0001$. Abbreviations: ANOVA, analysis of variance; AUC, area under the replication kinetic curve; hpi, hours postinfection; IAV, influenza A virus; IBV, influenza B virus; L, lung; NC, nasal cavity; PFU, plaque-forming unit; SP, soft palate; T, trachea; TCID₅₀, 50% tissue culture infection dose.

DISCUSSION

We showed in this study the limited permissiveness of canine respiratory and soft palate tissues to SARS-CoV-2 and SARS-CoV and their susceptibility to a wide range of human and avian influenza viruses. We also demonstrated the abundance of ACE2 receptors in the epithelia of canine nasal cavity and soft palate and of human and avian SA receptors in the epithelia of canine nasal cavity, soft palate, trachea, and lung.

While there was a slight trend of better replication of SARS-CoV-2 and SARS-CoV in canine nasal cavity and soft palate explants, the levels were far lower than expected considering the abundance of ACE2 in these tissues and the high similarity between human and canine ACE2, with efficient binding of SARS-CoV-2 receptor-binding domain (RBD) and SARS-CoV RBD proteins to canine ACE2 and transduction of SARS-CoV-2 and SARS-CoV pseudoviruses into cells expressing canine ACE2 [2, 27, 28]. In humans, there are 2 isoforms of ACE2, a functional full-length ACE2 (fACE2) and a nonfunctional Δ ACE2, which lacks the first 356 amino acid N-terminal region and thus is unable to bind to SARS-CoV-2 [29]. It is unknown if the

same applies to dogs and the ACE2 antibody used in our study cannot distinguish between the 2 isoforms. Future studies aimed at determining which of the ACE2 isoforms is detected by analyzing their mRNA and protein levels using qPCR, RNA-seq, immunoblotting, and maybe cytometric bead array assays are important in understanding SARS-CoV-2 and SARS-CoV infection and tropism. Coexpression of ACE2 and host activating proteases like furin and the transmembrane serine protease 2 (TMPRSS2), which are required for the proteolytic cleavage of SARS-CoV-2 spike protein for membrane fusion [30, 31], the degree to which dogs' cellular machinery supports SARS-CoV-2 replication, for example in terms of codon usage bias [32], and perhaps protection provided by the lower ACE2 expressions in the top cell layers of canine nasal cavity and soft palate epithelia may be critical restricting factors contributing to the low susceptibility of dogs to SARS-CoV-2 that need further investigations.

On the other hand, the susceptibility of the canine tissue explants to different human and avian influenza viruses matched with the abundance of both α 2,3- (avian) and α 2,6- (human)

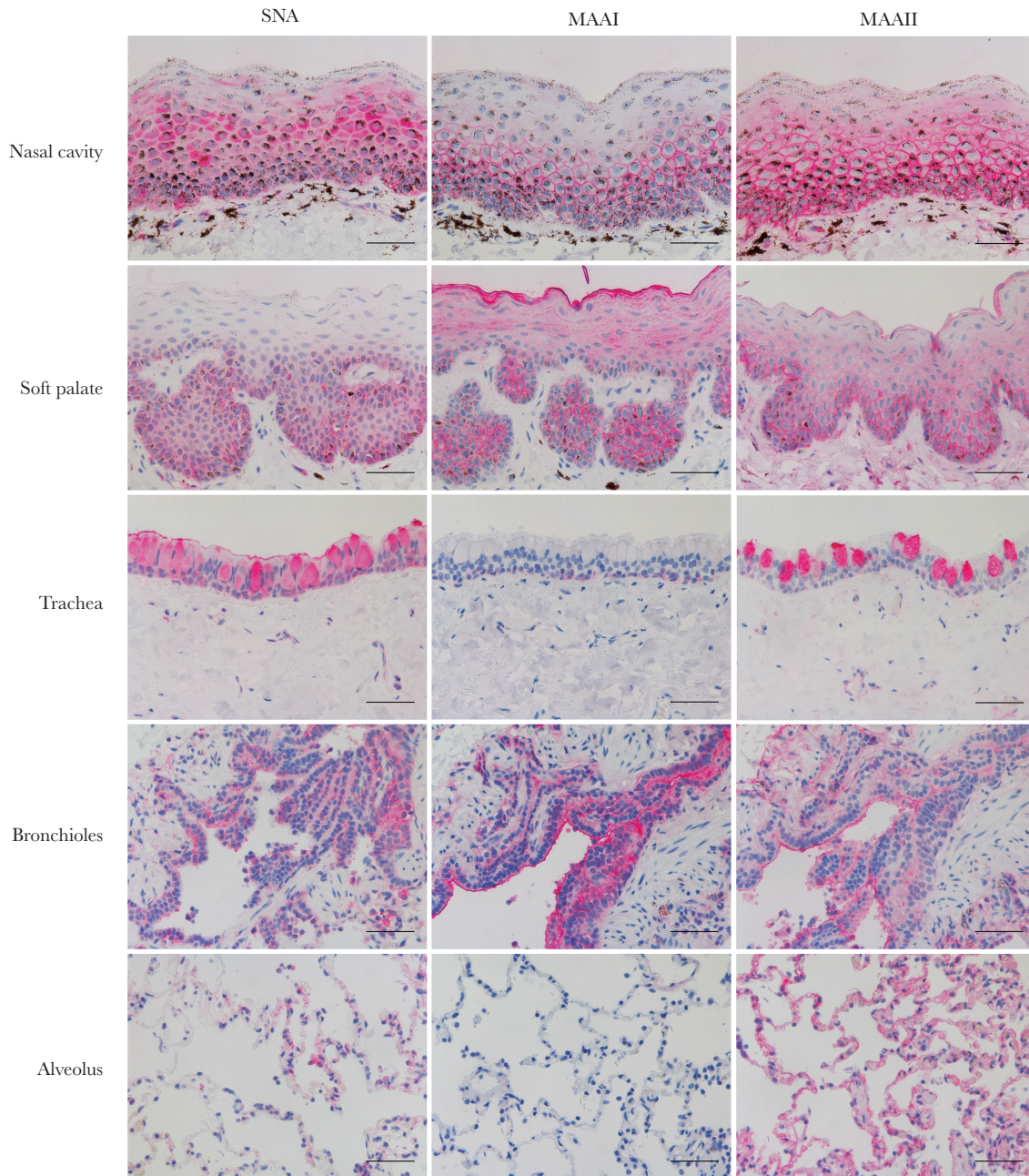


Figure 4. SA receptor distribution in canine respiratory and soft palate tissues. Binding (pinkish red) of SNA specific towards α 2,6-galactose linked SA, MAAI preferentially towards *N*-linked or core 2 *O*-linked glycans containing SA α 2,3-Gal β 1,4GlcNAc and non-SA glycans containing SO $_4$ -3-Gal β 1,4GlcNAc, and MAAII preferentially towards *O*-linked glycans containing SA α 2,3-Gal β 1,3GalNAc and non-SA glycans containing SO $_4$ -3-Gal β , in canine nasal cavity, soft palate, trachea, and lung (bronchioles and alveolus) tissue explants. Scale bars = 50 μ m. Abbreviations: MAAI, *Maackia amurensis* lectin I; MAAII, *Maackia amurensis* lectin II; SA, sialic acid; SNA, *Sambucus nigra* lectin.

galactose-linked SA receptors in the epithelia of these tissues. Existence of suitable receptors and tropism for the same tissue foster virus adaptation and reassortment, which could lead to the emergence of new viruses with potential threat. Natural reassortants between canine H3N2 and 2009 H1N1 pdm [33], avian H5N1 [34], and avian H9N2 [35] have been detected or isolated in dogs shortly after the emergence of canine H3N2. Hence, we were particularly concerned that HPAI H5 and H7 viruses and the highly prevalent avian H9N2 virus, which has been

shown to be a donor of internal genes to highly zoonotic viruses [36], had fairly high replication efficiencies in all canine tissues tested. Heterosubtypic reassortments may be more likely to occur in canine trachea and lung where most influenza subtypes in this study replicated well, providing greater chances of coinfections. Previously, higher genomic diversity was also found among reassortants recovered from the middle and lower respiratory tracts in experimental IAV coinfecting swine [37]. Nasal cavity and soft palate, which are highly exposed to the environment, have

been shown to be important sites of generation and adaptation for transmissible influenza viruses in ferrets [38, 39]. Whether the same applies to dogs remains to be answered. However, we demonstrated that canine nasal cavity and soft palate are among the initial sites of infection and amplification for human and avian influenza viruses. Higher viral loads at these sites could contribute in part to further dissemination through coughing, sneezing, breathing, and licking, as well as increased infection of the deeper tissues. However, it has to be noted that the physiological temperature in the canine nose at an ambient temperature of around 20°C is approximately 34°C, which is lower than the 37°C set for canine nasal cavity explants in our study. The difference in temperatures may lead to variations in viral replication at this site. Previous studies using the same strains of canine and human seasonal H3N2 and 2009 H1N1 pdm indicated similar to better replication efficiencies at 32–33°C than 37°C in primary human nasal and bronchial epithelial cells [16] and MDCK cells [40], respectively. The effect was the opposite for the replication of quail H9N2 in primary human bronchial epithelial cells [17] and the polymerase activity of HPAI H5N6 in 293T cells [41].

Although viral shedding of SARS-CoV-2 and SARS-CoV appears to be insufficient to cause efficient dissemination, the possibility of genetic recombination should be considered, given the many chances for spillover during outbreaks and the high prevalence of canine respiratory coronavirus, which belongs to the same beta-CoV genus, in dogs [42]. Coinfection between SARS-CoV-2 and influenza virus in dogs, as in humans [43], is another concern. The ways the 2 viruses interact and their influence on each other in replication, transmission, and pathogenesis is yet to be understood. One possible risk is the exposure of the more-vulnerable high-ACE2-expressing cell layers in canine nasal cavity and soft palate to SARS-CoV-2 after the initial damage by influenza virus infection.

Given the unique behavioral characteristics of dogs, their love to sniff and lick, and their height, there is increased risk of contamination from sick owners, infected animals, and the environment. Crowded places with poor hygiene condition, like live animal markets and dog meat farms, where dogs are found weakened, injured, and dehydrated, are the most concerning locations. In the context of the ongoing COVID-19 pandemic and the alarming zoonotic influenza outbreaks in the past, more precautionary measures and better surveillance should be implemented to protect dogs and prevent further infections as part of a successful global control. For example, dog meat farms, selling dog meat in live animal markets, and eating dog meat and should be prohibited. Sick or exposed owners should wear masks and practice good hygiene, or preferably be isolated from their dogs, until fully recovered and cleared of the disease. Similarly, sick or exposed dogs should be isolated, and their surrounding areas disinfected. Dogs could also be vaccinated with canine influenza vaccines if they are found to be at risk for exposure to the canine influenza virus.

To our knowledge, this is the first systematic comparison study of a large virus panel using all 4 relevant ex vivo canine respiratory and soft palate tissue explants. Considering the high level of consistency with previous surveillance and in vivo data [2, 20, 44–48], ex vivo canine tissue explants provide a reliable alternative to risk assess more viruses. Although transmission studies may only be completed with the use of live animals, ex vivo tissue explants can be used to assess virus infectivity first to avoid unnecessary pain and suffering of animals.

Supplementary Data

Supplementary materials are available at *The Journal of Infectious Diseases* online. Consisting of data provided by the authors to benefit the reader, the posted materials are not copyedited and are the sole responsibility of the authors, so questions or comments should be addressed to the corresponding author.

Notes

Acknowledgments. Our sincere thanks to Mr Kevin Fung (Department of Pathology, The University of Hong Kong, Hong Kong Special Administrative Region, China) for his assistance in immunohistochemistry; Ms Alfreda M.Y. Yuan, Ms Christy C.N. Chan, and Mr Richard T. C. Kung (Centre for Comparative Medicine Research, The University of Hong Kong) for their support in carcass dissection; Mr Jensen To (Department of Surgery, The University of Hong Kong) for technical support; and Dr K. H. Chan (Department of Microbiology, The University of Hong Kong), Dr Alexander Klimov (Influenza Division, Centers for Disease Control and Prevention, Atlanta, GA), and Dr I. J. Su (Tainan Virology Laboratory for Diagnosis and Research, Division of Clinical Research, National Health Research Institute, Tainan, Taiwan) for their generous sharing of virus seed stocks. We would also like to express our deepest gratitude to all the dogs whose carcasses were donated for the experiments. May they rest in peace.

Author contributions. C. H. T. B. designed and coordinated the study, did experiments, analyzed results, and wrote the manuscript. H. W. Y. and J. C. W. H. did experiments and analyzed results. C. Y. H. L. guided the carcass dissections. K. P. Y. H. and R. A. P. M. P. isolated SARS-CoV-2. R. J. W. and S. S.-C. provided H3N2 and HPAI H5N8 viruses. J. M. N. and J. S. M. P. designed the study, analyzed results, and reviewed the manuscript. M. C. W. C. contributed coordination and design of the study, analyzed results, and revised the manuscript.

Financial support. This work was supported by the Health and Medical Research Fund, Research Fund Secretariat, Food and Health Bureau, Hong Kong SAR, China (grant number 18171262); Research Grants Council, Hong Kong SAR, China, Theme Based Research Scheme (grant numbers T11-705/14N and T11-712/19-N); and the US National Institute of Allergy and Infectious Diseases, Centers of Excellence for Influenza Research and Surveillance (grant number HHSN272201400006C).

Potential conflicts of interest. All authors: No reported conflicts of interest. All authors have submitted the ICMJE Form for Disclosure of Potential Conflicts of Interest. Conflicts that the editors consider relevant to the content of the manuscript have been disclosed.

References

1. Chomel BB, Sun B. Zoonoses in the bedroom. *Emerg Infect Dis* **2011**; 17:167–72.
2. Sit THC, Brackman CJ, Ip SM, et al. Infection of dogs with SARS-CoV-2. *Nature* **2020**; 586:776–8.
3. Song D, Kang B, Lee C, et al. Transmission of avian influenza virus (H3N2) to dogs. *Emerg Infect Dis* **2008**; 14:741–6.
4. Lee YN, Lee DH, Lee HJ, et al. Evidence of H3N2 canine influenza virus infection before 2007. *Vet Rec* **2012**; 171:477.
5. Li S, Shi Z, Jiao P, et al. Avian-origin H3N2 canine influenza A viruses in southern China. *Infect Genet Evol* **2010**; 10:1286–8.
6. Voorhees IEH, Glaser AL, Toohey-Kurth K, et al. Spread of canine influenza A(H3N2) virus, United States. *Emerg Infect Dis* **2017**; 23:1950–7.
7. Xu W, Weese JS, Ojkic D, Lung O, Handel K, Berhane Y. Phylogenetic inference of H3N2 canine influenza A outbreak in Ontario, Canada in 2018. *Sci Rep* **2020**; 10:6309.
8. Su W, Kinoshita R, Gray J, et al. Seroprevalence of dogs in Hong Kong to human and canine influenza viruses. *Vet Rec Open* **2019**; 6:e000327.
9. Sun Y, Shen Y, Zhang X, et al. A serological survey of canine H3N2, pandemic H1N1/09 and human seasonal H3N2 influenza viruses in dogs in China. *Vet Microbiol* **2014**; 168:193–6.
10. Jang H, Jackson YK, Daniels JB, et al. Seroprevalence of three influenza A viruses (H1N1, H3N2, and H3N8) in pet dogs presented to a veterinary hospital in Ohio. *J Vet Sci* **2017**; 18:291–8.
11. Smith GJ, Vijaykrishna D, Bahl J, et al. Origins and evolutionary genomics of the 2009 swine-origin H1N1 influenza A epidemic. *Nature* **2009**; 459:1122–5.
12. Ma W, Kahn RE, Richt JA. The pig as a mixing vessel for influenza viruses: human and veterinary implications. *J Mol Genet Med* **2008**; 3:158–66.
13. Bui CHT, Chan RWY, Ng MMT, et al. Tropism of influenza B viruses in human respiratory tract explants and airway organoids. *Eur Respir J* **2019**; 54:1900008.
14. Hui KPY, Cheung MC, Perera RAPM, et al. Tropism, replication competence, and innate immune responses of the coronavirus SARS-CoV-2 in human respiratory tract and conjunctiva: an analysis in ex-vivo and in-vitro cultures. *Lancet Respir Med* **2020**; 8:687–95.
15. Hui KP, Chan LL, Kuok DI, et al. Tropism and innate host responses of influenza A/H5N6 virus: an analysis of ex vivo and in vitro cultures of the human respiratory tract. *Eur Respir J* **2017**; 49:1601710.
16. Martinez-Sobrido L, Blanco-Lobo P, Rodriguez L, et al. Characterizing emerging canine H3 influenza viruses. *PLoS Pathog* **2020**; 16:e1008409.
17. Mok CK, Yen HL, Yu MY, et al. Amino acid residues 253 and 591 of the PB2 protein of avian influenza virus A H9N2 contribute to mammalian pathogenesis. *J Virol* **2011**; 85:9641–5.
18. Chan LL, Bui CT, Mok CK, et al. Evaluation of the human adaptation of influenza A/H7N9 virus in PB2 protein using human and swine respiratory tract explant cultures. *Sci Rep* **2016**; 6:35401.
19. Gonzalez G, Marshall JF, Morrell J, et al. Infection and pathogenesis of canine, equine, and human influenza viruses in canine tracheas. *J Virol* **2014**; 88:9208–19.
20. Shi J, Wen Z, Zhong G, et al. Susceptibility of ferrets, cats, dogs, and other domesticated animals to SARS-coronavirus 2. *Science* **2020**; 368:1016–20.
21. Korber B, Fischer WM, Gnanakaran S, et al; Sheffield COVID-19 Genomics Group. Tracking changes in SARS-CoV-2 spike: evidence that D614G increases infectivity of the COVID-19 virus. *Cell* **2020**; 182:812–27.e19.
22. Toyoshima Y, Nemoto K, Matsumoto S, Nakamura Y, Kiyotani K. SARS-CoV-2 genomic variations associated with mortality rate of COVID-19. *J Hum Genet* **2020**; 65:1075–82.
23. Phan T. Genetic diversity and evolution of SARS-CoV-2. *Infect Genet Evol* **2020**; 81:104260.
24. Maitra A, Sarkar MC, Raheja H, et al. Mutations in SARS-CoV-2 viral RNA identified in Eastern India: possible implications for the ongoing outbreak in India and impact on viral structure and host susceptibility. *J Biosci* **2020**; 45:76.
25. Nicholls JM, Bourne AJ, Chen H, Guan Y, Peiris JS. Sialic acid receptor detection in the human respiratory tract: evidence for widespread distribution of potential binding sites for human and avian influenza viruses. *Respir Res* **2007**; 8:73.
26. Geisler C, Jarvis DL. Effective glycoanalysis with *Maackia amurensis* lectins requires a clear understanding of their binding specificities. *Glycobiology* **2011**; 21:988–93.
27. Wu L, Chen Q, Liu K, et al. Broad host range of SARS-CoV-2 and the molecular basis for SARS-CoV-2 binding to cat ACE2. *Cell Discov* **2020**; 6:68.
28. Zhai X, Sun J, Yan Z, et al. Comparison of severe acute respiratory syndrome coronavirus 2 spike protein binding to ACE2 receptors from human, pets, farm animals, and putative intermediate hosts. *J Virol* **2020**; 94:e00831-20.
29. Zamorano Cuervo N, Grandvaux N. ACE2: evidence of role as entry receptor for SARS-CoV-2 and implications in comorbidities. *Elife* **2020**; 9:e61390.

30. Bestle D, Heindl MR, Limburg H, et al. TMPRSS2 and furin are both essential for proteolytic activation of SARS-CoV-2 in human airway cells. *Life Sci Alliance* **2020**; 3:e202000786.
31. Hoffmann M, Kleine-Weber H, Schroeder S, et al. SARS-CoV-2 cell entry depends on ACE2 and TMPRSS2 and is blocked by a clinically proven protease inhibitor. *Cell* **2020**; 181:271–80.e8.
32. Tian L, Shen X, Murphy RW, Shen Y. The adaptation of codon usage of +ssRNA viruses to their hosts. *Infect Genet Evol* **2018**; 63:175–9.
33. Na W, Lyoo KS, Song EJ, et al. Viral dominance of reassortants between canine influenza H3N2 and pandemic (2009) H1N1 viruses from a naturally co-infected dog. *Virol J* **2015**; 12:134.
34. Zhu H, Hughes J, Murcia PR. Origins and evolutionary dynamics of H3N2 canine influenza virus. *J Virol* **2015**; 89:5406–18.
35. Lee IH, Le TB, Kim HS, Seo SH. Isolation of a novel H3N2 influenza virus containing a gene of H9N2 avian influenza in a dog in South Korea in 2015. *Virus Genes* **2016**; 52:142–5.
36. Peacock THP, James J, Sealy JE, Iqbal M. A global perspective on H9N2 avian influenza virus. *Viruses* **2019**; 11:620.
37. Zhang X, Sun H, Cunningham FL, et al. Tissue tropisms opt for transmissible reassortants during avian and swine influenza A virus co-infection in swine. *PLoS Pathog* **2018**; 14:e1007417.
38. Richard M, van den Brand JMA, Bestebroer TM, et al. Influenza A viruses are transmitted via the air from the nasal respiratory epithelium of ferrets. *Nat Commun* **2020**; 11:766.
39. Lakdawala SS, Jayaraman A, Halpin RA, et al. The soft palate is an important site of adaptation for transmissible influenza viruses. *Nature* **2015**; 526:122–5.
40. Wang P, Zheng M, Lau SY, et al. Generation of DelNS1 influenza viruses: a strategy for optimizing live attenuated influenza vaccines. *mBio* **2019**; 10:e02180-19.
41. Herfst S, Mok CKP, van den Brand JMA, et al. Human clade 2.3.4.4 A/H5N6 influenza virus lacks mammalian adaptation markers and does not transmit via the airborne route between ferrets. *mSphere* **2018**; 3:e00405-17.
42. Erles K, Brownlie J. Canine respiratory coronavirus: an emerging pathogen in the canine infectious respiratory disease complex. *Vet Clin North Am Small Anim Pract* **2008**; 38:815–25, viii.
43. Cuadrado-Payán E, Montagud-Marrahi E, Torres-Elorza M, et al. SARS-CoV-2 and influenza virus co-infection. *Lancet* **2020**; 395:e84.
44. Song D, Kim H, Na W, et al. Canine susceptibility to human influenza viruses (A/pdm 09H1N1, A/H3N2 and B). *J Gen Virol* **2015**; 96:254–8.
45. Lin D, Sun S, Du L, et al. Natural and experimental infection of dogs with pandemic H1N1/2009 influenza virus. *J Gen Virol* **2012**; 93:119–23.
46. Chen Y, Zhong G, Wang G, et al. Dogs are highly susceptible to H5N1 avian influenza virus. *Virology* **2010**; 405:15–9.
47. Songserm T, Amonsin A, Jam-on R, et al. Fatal avian influenza A H5N1 in a dog. *Emerg Infect Dis* **2006**; 12:1744–7.
48. Zhang K, Zhang Z, Yu Z, et al. Domestic cats and dogs are susceptible to H9N2 avian influenza virus. *Virus Res* **2013**; 175:52–7.